Sixth International Symposium on Turbulence and Shear Flow Phenomena
Seoul, Korea, 22-24 June 2009

# INVESTIGATION OF TURBULENT BOUNDARY LAYER OVER FORWARD-FACING STEP BY MEANS OF DNS

**Hirofumi Hattori**
Department of Mechanical Engineering,
Nagoya Institute of Technology
Gokiso-cho, Showa-ku, Nagoya, 466-8555, Japan
hattori@heat.mech.nitech.ac.jp

**Yasutaka Nagano**
Department of Mechanical Engineering,
Nagoya Institute of Technology
nagano@heat.mech.nitech.ac.jp

## ABSTRACT

This paper presents observations and investigations of the detailed structure of a turbulent boundary layer over a forward-facing step. A turbulent boundary layer with reattachment and separation which causes an increase in friction of flow and disturbance in transportation of scalar often occurs in fluid machinery, the atmosphere, etc. Thus, it is important for friction reduction and environmental protection to know the transport phenomena of a boundary layer with reattachment and separation. However, little data on a boundary layer with reattachment and separation are available in comparison with an internal turbulent flow such as a channel flow. Data of turbulent heat and mass transfer in the boundary layer over a block are especially difficult to obtain. Therefore, in order to investigate the detailed turbulent quantities of a boundary layer over an obstacle which causes reattachment and separation, a DNS of the turbulent boundary layer over a forward-facing step must first be carried out. The present DNSs are conducted under conditions with various Reynolds numbers based on step height, or based on momentum thickness so as to investigate the effects of step height and inlet boundary layer thickness. DNS results show the quantitative turbulent statistics and structures of boundary layers over a forward-facing step, in which the characteristic transport phenomena in the recirculation regions which occur in front of and on the step are demonstrated.

## INTRODUCTION

The authors have been conducting DNSs of a boundary layer (Hattori *et al.*, 2007), in which understanding of the turbulence phenomena in the thermally stratified boundary layer has been improved, and a flow database has been constructed. The turbulent characteristic of the thermally stratified boundary layer is investigated in detail, and the prediction performance of turbulence models is evaluated using DNS in order to improve the turbulence model for prediction of turbulent flows. Additionally, we need to conduct DNS concerning more complicated turbulence such as a turbulent flow over an obstacle which is modeled as the typical flow in a complex flow field and causes flow reattachment of separation, to comprehend transport phenomena there. A turbulent boundary layer with reattachment and separation has been observed in hydrodynamic phenomena, which with turbulence become more complex. Since the reattachment and separation of flow causes an increase in friction of flow and disturbance in transport of scalar, the hydrodynamic phenomena in a turbulent flow with reattachment and separation should be investigated in detail so as to decrease friction and enhance transport of scalar. A typical flow with reattachment and separation is a back-ward facing step flow, and many studies has been reported by both experiment and calculation (e.g., Kasagi and Matsunaga, 1995; Le *et al.*, 1997; Vogel and Eaton, 1985). Thus, the most notable separated flow is a back-ward facing step flow. On the other hand, a flow which causes reattachment and separation includes a forward-facing step flow, but useful detailed data including turbulence are scarce (e.g., Moss and Baker, 1980; Shakouchi *et al.*, 1999). Since a forward-facing step flow occurs in various flow situations, we should know the detailed turbulent phenomena, flow properties and structures. Therefore the objective of this study is to investigate turbulent boundary layers over a forward-facing step. In such flows, however, it is difficult to predict and measure distributions of turbulence, since various types of machinery, building structures and terrain complicate transport phenomena of the kind. Hence, direct numerical simulation (DNS) is a very useful and powerful technique in order to determine such detailed turbulence phenomena as well as experimental techniques. Especially, the near-wall turbulent structure can be clarified by DNS. Thus, DNS of the turbulent boundary layer over a forward-facing step is carried out to obtain detailed knowledge of the effect of the forward-facing step in various Reynolds numbers. In particular, transport phenomena near the step are selectively explored.

## NUMERICAL PROCEDURE

The governing equations used in DNS are the Navier-Stokes equation without buoyancy, the continuity equation for the velocity field, and the energy equation for the thermal field, in which incompressibility is assumed as follows:

$$\frac{\partial u_i^*}{\partial x_i^*} = 0 \tag{1}$$

$$\frac{\partial u_i^*}{\partial t^*} + u_j^* \frac{\partial u_i^*}{\partial x_j^*} = -\frac{\partial p^*}{\partial x_i^*} + \frac{1}{Re_{\delta_{2,\mathrm{in}}}} \frac{\partial^2 u_i^*}{\partial x_j^* \partial x_j^*} \tag{2}$$

where the Einstein summation convention applies to re-

Table 1: Computational method and conditions

| | | |
|---|---|---|
| Grid | Staggered Grid | |
| Coupling Algorithm | Fractional Step Method | |
| Time Advancement | Adams-Bashforth Method | |
| Spatial schemes | 2nd-order central difference | |
| Domain size | Driver | $100\delta_{2,\mathrm{in}} \times 30\delta_{2,\mathrm{in}} \times 40\delta_{2,\mathrm{in}}$ |
| $(x \times y \times z)$ | Main | $100\delta_{2,\mathrm{in}} \times 30\delta_{2,\mathrm{in}} \times 40\delta_{2,\mathrm{in}}$ |
| $Re_h = 900, 1800$ | Driver | $192 \times 128 \times 128$ |
| Grid numbers $(x \times y \times z)$ | Main | $288 \times 128 \times 128$ |
| $Re_h = 3000$ | Driver | $192 \times 256 \times 256$ |
| Grid numbers $(x \times y \times z)$ | Main | $576 \times 256 \times 256$ |

Table 2: Separation and reattachment points

| $Re_h$ | $h$ | Sepa. point $(x/h)$ | Reat. point $(x/h)$ |
|---|---|---|---|
| 900 | $3\delta_{2,\mathrm{in}}$ | $-1.91$ | 2.04 |
| 1800 | $3\delta_{2,\mathrm{in}}$ | $-1.81$ | 1.82 |
| 1800 | $6\delta_{2,\mathrm{in}}$ | $-1.93$ | 1.86 |
| 3000 | $3\delta_{2,\mathrm{in}}$ | $-1.73$ | 2.01 |

peated indices, and a comma followed by an index indicates differentiation with respect to the indexed spatial coordinate. $u_i^*$ is the dimensionless velocity component in $x_i$ direction, $p^*$ is the dimensionless pressure, $t^*$ is the dimensionless time, and $x_i^*$ is the dimensionless spatial coordinate in the $i$ direction, respectively. All equations are non-dimensionalized by the free stream velocity, $\bar{U}_0$, and the momentum thickness, $\delta_{2,\mathrm{in}}$, at the inlet of the driver part. Figure 1 shows a schematic of the forward-facing step and the coordinate system. The present DNS based on the high-accuracy finite-difference method (Hattori *et al.*, 2007) is carried out under conditions of Reynolds numbers based

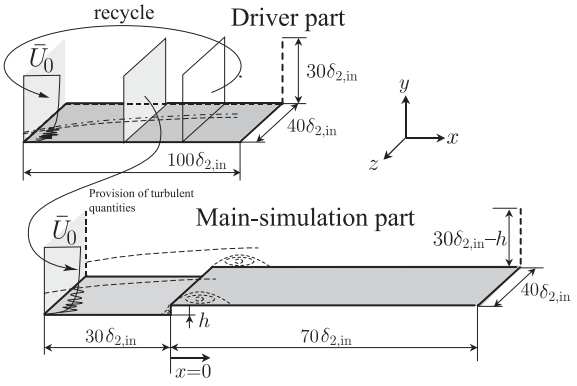


Figure 1: Coordinate system

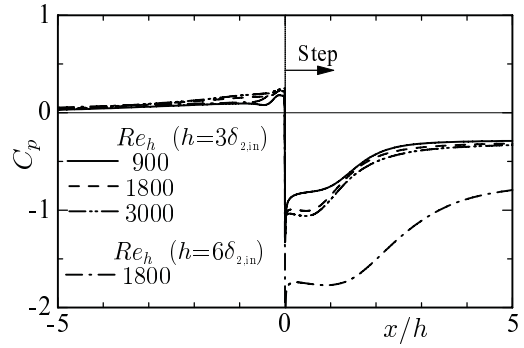


Figure 2: Distributions of pressure coefficients

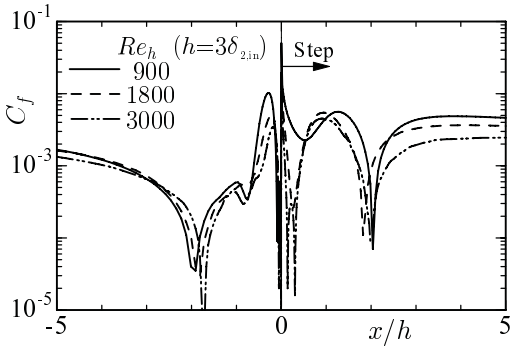


(a) $h = 3\delta_{2,\mathrm{in}}$

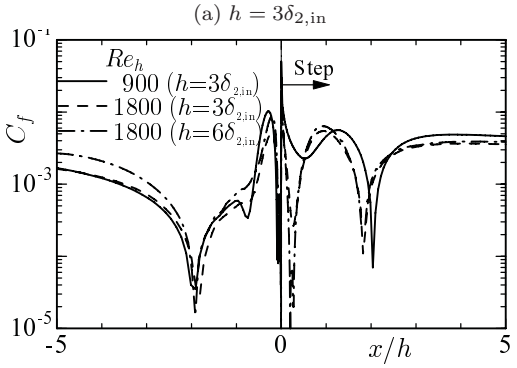


(b) $h = 3\delta_{2,\mathrm{in}}, 6\delta_{2,\mathrm{in}}$

Figure 3: Distributions of friction coefficients

on the free stream velocity and the momentum thickness at the inlet of the driver part, $Re_{\delta_{2,\mathrm{in}}}$=300, 600 and 1000, in order to explore the influence of the Reynolds number in the present condition. The step height, $h$, is fundamentally set to $3\delta_{2,\mathrm{in}}$, but is also set to $6\delta_{2,\mathrm{in}}$ in the case of $Re_{\delta_{2,\mathrm{in}}}$=300 in order to observe the effect of the step height on turbulence. These heights are about $1/3 \sim 2/3$ of the boundary layer thickness at the inlet of the driver. Thus, the Reynolds numbers based on the step height become $Re_h = 900 \sim 3000$. Note that the Reynolds number based on the momentum thickness is used in the calculation, but the Reynolds number based on the step height is employed in the result, because the proper Reynolds number which may represent a forward-facing step flow is $Re_h$. The detailed computational method and conditions include the algorithm, domain size and grid numbers of DNS. The boundary conditions for the velocity field are the non-slip conditions on the walls, and $\partial u/\partial y = 0$, $\partial w/\partial y = 0$, $\partial v/\partial y = -(\partial u/\partial x + \partial w/\partial z)$ on the upper boundary (free stream). At the outlet of both parts, convective boundary conditions are applied, and periodic boundary conditions are used in the spanwise direction.

## RESULTS AND DISCUSSION

### Fundamental Flow Properties

First, the fundamental flow properties of present boundary layer over a forward-facing step are shown. Figure 2 shows the pressure coefficients around the step in all cases. Obviously, the case of step height $h = 6\delta_{2,\mathrm{in}}$ indicates a dissimilar distribution in comparison with the step height $h = 3\delta_{2,\mathrm{in}}$ of the step. On the other hand, the distributions of friction coefficients of the case of the step height $h = 3\delta_{2,\mathrm{in}}$ are shown in Fig. 3(a) and the case of the step

height $h = 6\delta_{2,\mathrm{in}}$, in which the cases of $Re_h = 300$ and $= 600$ with the step height $h = 3\delta_{2,\mathrm{in}}$ are included for comparison, are shown in Fig. 3(b). Also, the separation points in front of the step and the reattachment points on the step are listed in Tab. 2. The nearest separation point from the step is given in the case of the highest Reynolds number, $Re_h = 3000$, and the longest reattachment point on the step is obtained in the case of the lowest Reynolds number, $Re_h = 900$. The experimental result (Moss and Baker, 1980; $Re_h$=50,000) indicated $-1.50 \sim -1.00$ for the detachment point and 4.70 for the reattachment point. The obvious reason for this disagreement is the Reynolds number difference. In particular, the step height in comparison with the boundary layer thickness of the experiment is higher than that of the DNS, i.e., the step height exceeds the boundary layer thickness in the experiment, but the step height of all cases of present DNSs are within the boundary layer thickness.

As for the distribution of friction coefficient, the case of $Re_h = 900$ gives a dissimilar distribution in comparison with the other cases on the step near the corner. However, no clear difference in distributions of friction coefficients in the other cases can be found. In order to investigate the flow situation, the streamlines around the step of all cases are shown in Fig. 4. It is well-known that the separation regions occur in front of and on the step in the forward-facing step flow. The present DNSs obviously represent the

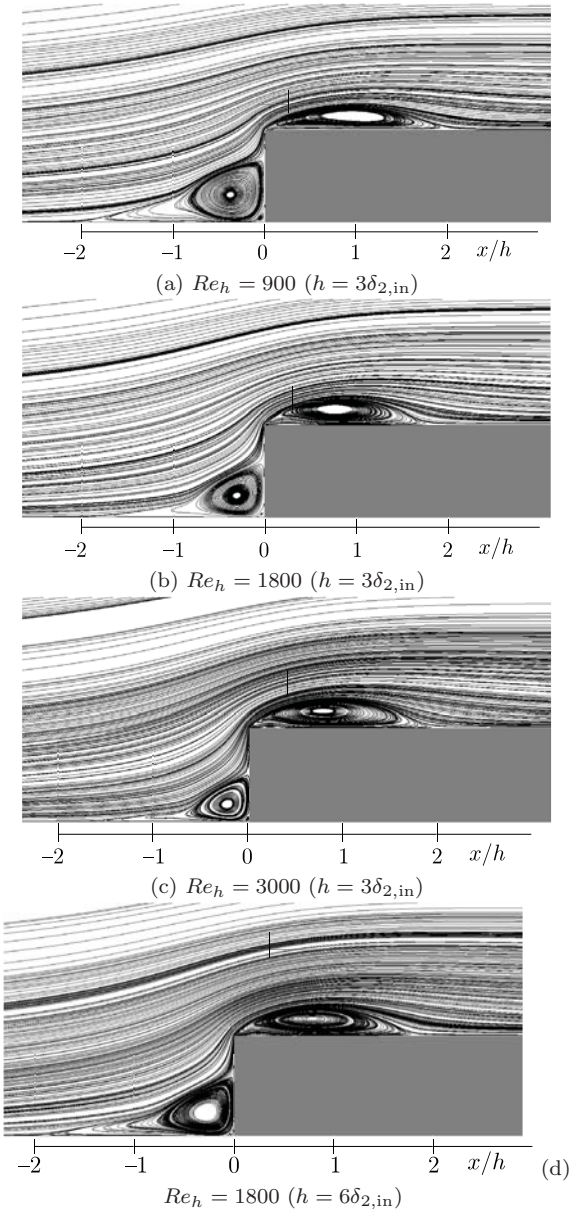


Figure 4: Streamlines around the step

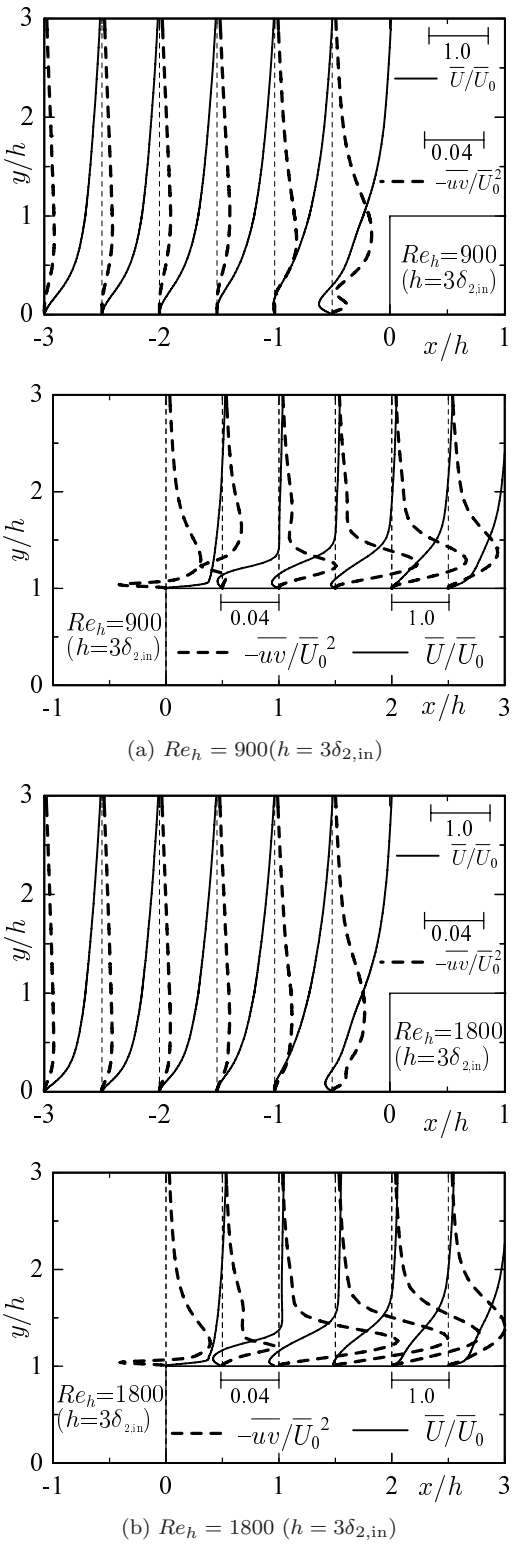


Figure 5: Near-wall profiles of streamwise mean velocity and Reynolds shear stress around the step

characteristic flow configuration of forward-facing step flow. The smallest separation region in front of the step can be observed in the case of $Re_h = 3000$. Thus, the nearest separation point from the step is given in this case. On the other hand, the separation region on the step in the case of $Re_h = 900$ reveals a can be observed slight difference. Thus, dissimilar distributions of friction coefficients of the case are given in comparison with the other cases.

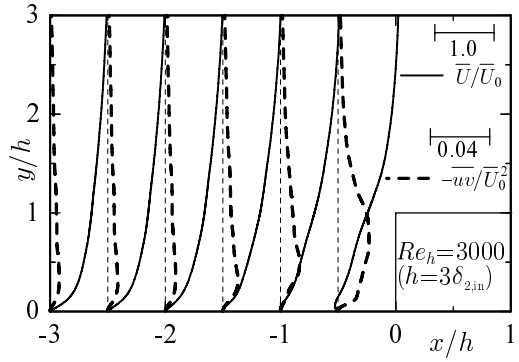


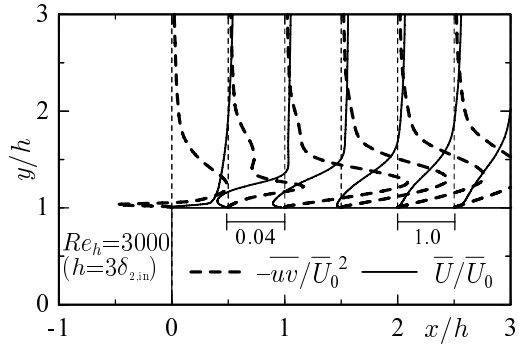


(c) $Re_h = 3000$ ($h = 3\delta_{2,\mathrm{in}}$)

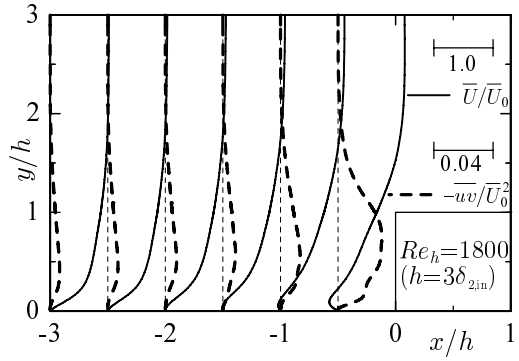


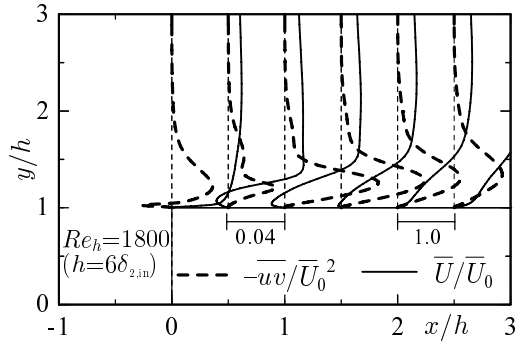


(d) $Re_h = 1800$ ($h = 6\delta_{2,\mathrm{in}}$)

Figure 5: (continued)

### Turbulent Statistics

The near-wall profiles of streamwise mean velocities and Reynolds shear stresses in front of and on the step are shown in Fig. 5. The mean velocities of the case of $Re_h = 1800$ with the step height $h = 6\delta_{2,\mathrm{in}}$ remarkably accelerate on the step

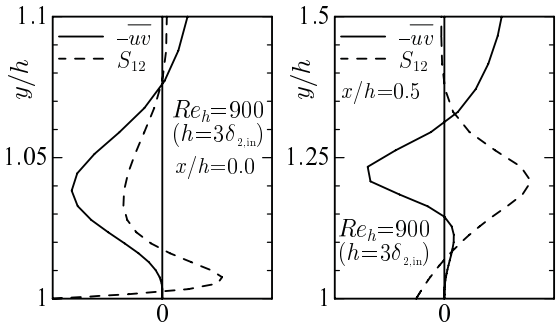


(a) $Re_h = 900$ ($h = 3\delta_{2,\mathrm{in}}$)

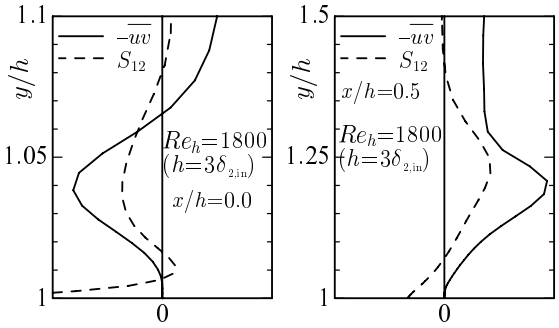


(b) $Re_h = 1800$ ($h = 3\delta_{2,\mathrm{in}}$)

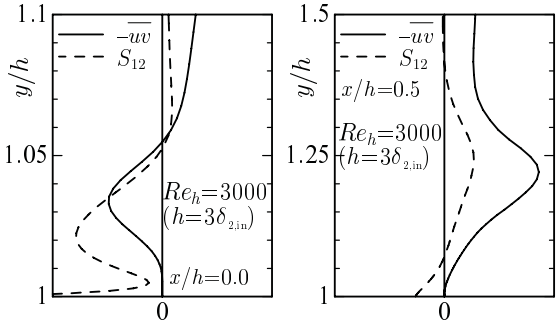


(c) $Re_h = 3000$ ($h = 3\delta_{2,\mathrm{in}}$)

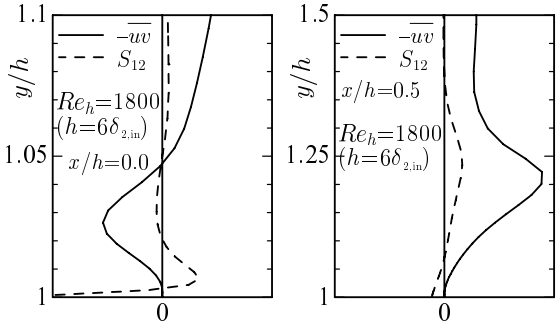


(d) $Re_h = 1800$ ($h = 6\delta_{2,\mathrm{in}}$)

Figure 6: Relations between Reynolds shear stress and mean velocity gradient in vicinity of the wall

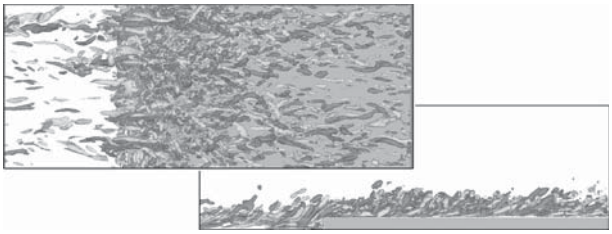

(a) $Re_h = 900$ ($h = 3\delta_{2,\mathrm{in}}$)

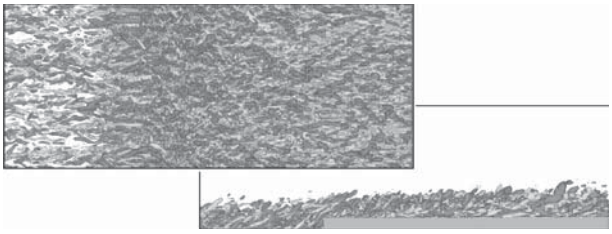

(b) $Re_h = 1800$ ($h = 3\delta_{2,\mathrm{in}}$)

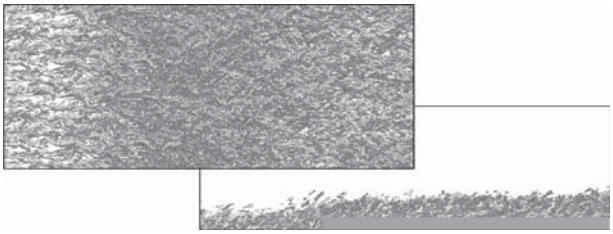

(c) $Re_h = 3000$ ($h = 3\delta_{2,\mathrm{in}}$)

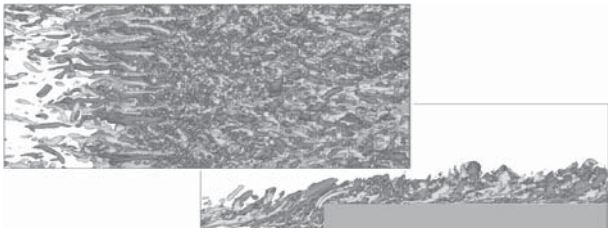

(d) $Re_h = 1800$ ($h = 6\delta_{2,\mathrm{in}}$)

Figure 7: Vortex structures around the step

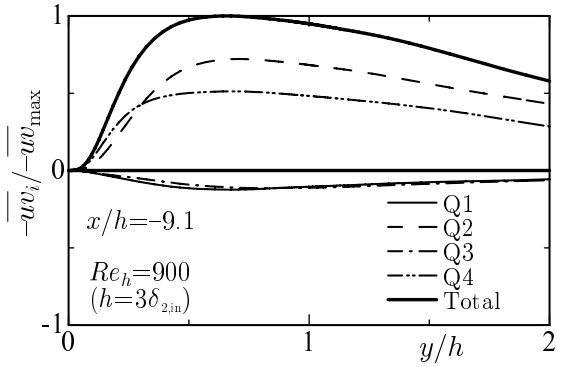


Figure 8: Fractional contributions of different quadrant motions at inlet boundary layer

due to higher step height than that of the other cases. The Reynolds shear stress increases near the wall on the step due to the increase in the shear of the mean velocity. Also, the Reynolds shear stress increases in front of the step, where the separation region causing the increase in the shear of the mean velocity exists. Since the different distribution

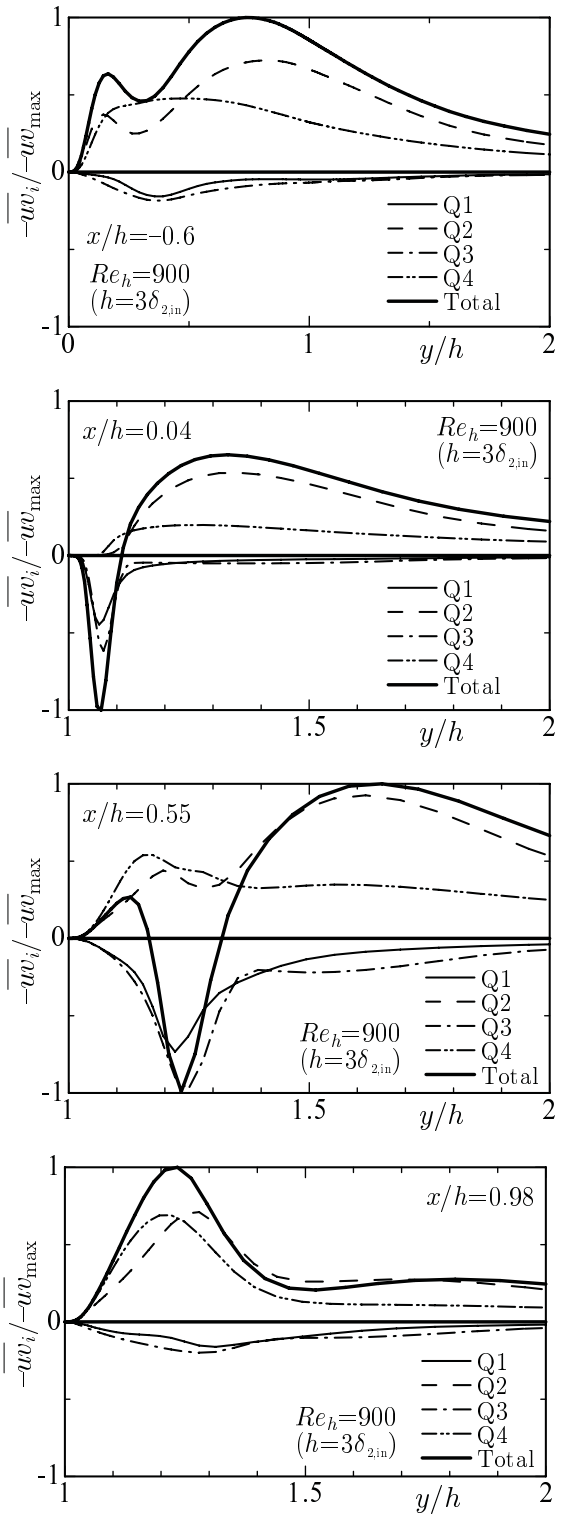


Figure 9: Fractional contributions of different quadrant motions around the step

of Reynolds shear stresses is found in the case around the step, it can be considered that the dissimilar distribution of friction coefficients is given.

It can be found that the counter gradient diffusion phenomenon (CGDP) between the streamwise mean velocity and Reynolds shear stress appears near the corner of the step ($x/h \sim 0$). Especially, the CGDP remarkably ap-

pears in the case of the lowest Reynolds number. Note that we define the CGDP as the opposite sign between the Reynolds shear stress, $-\overline{uv}$, and the mean velocity gradient, $S_{12} = \partial\bar{U}/\partial y + \partial\bar{V}/\partial x$, simultaneously occur. Although it can be seen that the profiles of both Reynolds shear stress and streamwise mean velocity are almost similar on the step in all cases as indicated in Fig. 5, $S_{12}$ of the case of the highest Reynolds number gives the negative sign as indicated in Fig. 6(c). Thus, the CGDP on the step is less apt to occur as the Reynolds number increases. In the downstream of the corner $x/h = 0.5$, the CGDP appears in the vicinity of the wall in all cases, but the CGDP vanishes at the region away from the wall in the case of higher Reynolds number than the case of $Re_h = 900$ as shown in Fig. 6.

### Turbulent Structures and Quadrant Analysis

From investigating the turbulent structure of the boundary layer over the forward-facing step in detail, the vortex structures around the step may be shown as in Fig. 7, where the vortex structure is determined by the second invariant of the velocity gradient. It can be seen that the vortex structure develops due to the effect of the step toward downstream direction on the step in all cases, where the continuous vortex structure can be observed clearly. With an increase in Reynolds number, the vortex structure obviously becomes fine, and the step causes production of a finer vortex than that in front of the step. In the case of the lowest Reynolds number, however, a discontinuous vortex structure appears over the recirculation region due to the boundary layer redevelopment. With an increase in step height, the vortex structure is promoted more than the case of $Re_h = 900$ whose inlet condition of boundary layer is identical with the case of the highest step. The effect of the step obviously influences the redevelopment of the boundary layer in the downstream region.

Finally, a quadrant analysis (Nagano and Tagawa, 1988) is conducted to investigate in detail turbulence motion around the step. Such analysis is especially used to explore the case of the lowest Reynolds number, in which the CGDP remarkably occurs. In general, the Q2 motion (ejection) and the Q4 motion (sweep) dominate the production of Reynolds shear stress in the wall turbulent shear flow as indicated in Fig. 8. Note that the motions are normalized by the maximum Reynolds shear stress at the point, and the total means the Reynolds shear stress itself. In particular, the Q4 motion dominates near the wall, and the Q2 motion affects the region away from the wall for the Reynolds shear stress. Figures 9 show the fractional contributions of different quadrant motions around the step. At $x/h = -0.6$, which is the recirculation region in front of the step, the Reynolds shear stress has three inflection points, in which the Q2 motion is similar in the profile of Reynolds shear stress. At such points, the Q4 motion increases near the wall, but the Q1 (outward interaction) and Q3 (wallward interaction) motions influence the Reynolds shear stress. Thus, the Reynolds shear stress decreases near the wall, whereas the Q4 motion increases. On the step near the corner ($x/h = 0.04$) in which the CGDP appears, the Q1 and Q3 motions remarkably affect the negative Reynolds shear stress. The Q3 motion especially contributes to the region where the Reynolds shear stress indicates a negative sign. In the region away from the wall, the Q2 motion dominates as the usual wall turbulent shear flow. At the downstream point in the recirculation region on the step ($x/h = 0.55$), the profiles of Reynolds shear stress significantly vary. In the vicinity of the wall at $x/h = 0.55$, the Q4 motion is observed as the dominative motion. The Q3 motion becomes the dominative motion in the region where the Reynolds shear stress indicates the negative sign. At the point ($x/h = 0.98$) where the Reynolds shear stress completely indicates the positive sign, the dominative motion is similar in the usual wall turbulent shear flow as indicated in Fig. 8, but the dominative region of Q4 becomes wide near the wall.

## CONCLUSIONS

DNSs of turbulent boundary layers over forward-facing step are carried out to investigate in detail the transport phenomena of such flows. The present DNS indicates the fundamental and detailed characteristics of turbulent boundary layers over a forward-facing step under various step and flow conditions. In particular, pronounced counter-gradient diffusion phenomena (CGDP) are observed. Therefore, it is concluded that the obvious turbulent boundary layer over the forward-facing step can be investigated in detail by means of DNS. Also, DNS of a higher Reynolds number is carried out in order to investigate the Reynolds number dependence of such flows. With an increase in Reynolds number, the CGDP is less apt to occur. Thus, the CGDP appears remarkably in the case of a small Reynolds number. On the other hand, in order to investigate turbulence motion around the step in detail, quadrant analysis is conducted. The quadrant analysis clearly shows the dominative motion for the production of Reynolds shear stress around the step. Therefore, we can observe and investigate the detailed structure of a turbulent boundary layer over a forward-facing step.

## ACKNOWLEDGEMENT

This research was supported by a Grant-in-Aid for Scientific Research (S), 17106003, from the Japan Society for the Promotion of Science (JSPS).

## REFERENCES

Hattori, H., Houra, T. and Nagano, Y., 2007, Direct numerical simulation of stable and unstable turbulent thermal boundary layers. *Int. J.Heat and Fluid Flow*, **28**, pp.1262–1271.

Kasagi, N., and Matsunaga, A., 1995, Three-dimensional particle-tracking velocimetry measurement of turbulence statistics and energy budget in a backward-facing step flow. *Int. J. Heat Fluid Flow*, **16** pp. 477–485.

Le, H., Moin, P., and Kim, J., 1997, Direct numerical simulation of turbulent flow over a backward-facing step. *J. Fluid Mechanics*, **330**, pp.349–374.

Moss, W. D. and Baker, S., 1980, Re-circulating flow associated with two-dimensional steps. *Aeronautical Quarterly*, August, pp.151-172.

Nagano, Y. and Tagawa, M., 1988, Statistical characteristics of wall turbulence with passive scalar. *J. Fluid Mechanics*, **196**, pp.157–185.

Shakouchi, T. Ando, T., and Nakano K., 1999, Flow characteristics over forward facing step and control of separated flow. *Trans.JSME, Ser. B*, **65**, pp.3008–3014.

Vogel, J. C., and Eaton, J. K., 1985, Combined heat transfer and fluid dynamic measurements downstream of a backward-facing step. *Trans. ASME, J. Heat Transfer*, **107**, pp. 922–929.